# Elucidating the Crystal Structure of DL-Arginine by Combined Powder X-ray Diffraction Data Analysis and Periodic DFT-D Calculations

Colan E. Hughes, Ines Boughdiri, Clément Bouakkaz, P. Andrew Williams and Kenneth D. M. Harris*

School of Chemistry, Cardiff University, Park Place, Cardiff, CF10 3AT, U.K.

* Author for correspondence: HarrisKDM@cardiff.ac.uk

Dedicated to Professor William Jones (University of Cambridge) in recognition of his wide-ranging contributions to Organic Solid-State Chemistry

## Abstract

Among the 20 directly-encoded proteinogenic amino acids, arginine is one of five remaining cases for which the crystal structure of a racemic crystalline phase has not yet been reported. In this paper, the crystal structure of DL-arginine is determined by exploiting modern methods for analysis of powder X-ray diffraction data, in conjunction with periodic DFT-D calculations. The crystal structure of DL-arginine provides interesting contrasts and comparisons to that of the enantiomerically pure crystalline phase (L-arginine), which was also determined recently from powder X-ray diffraction data.

## Introduction

While there is significant interest in the solid-state properties of the 20 directly-encoded proteinogenic amino acids, it is only very recently that the crystal structures of the enantiomerically pure forms have been reported for all members of this family.[1] Following the first crystal structure determination[2] of an amino acid in this family in 1939, it took over 70 years before the crystal structures of the enantiomerically pure forms of all 19 chiral amino acids in this family were determined, with the reported crystal structure determinations of L-arginine[3] and L-tryptophan[4] in 2013, and L-lysine[5] in 2015. Furthermore, within the last few years, a completely new understanding of the polymorphic landscape for L-phenylalanine has emerged, with the discovery of three new polymorphs[6-7] and revision of the structure of the only previously known form.[7]

In contrast, there has been significantly less progress in establishing the crystal structures of racemate crystalline forms (in which both the R-enantiomer and the S-enantiomer are present in equal amounts within the crystal structure). Of the 19 chiral members of the set, racemate crystal structures are known in 14 cases, the most recently reported of which were DL-isoleucine[8] in 2000 and a second polymorph of DL-cysteine[9] (at low temperature) in 2009. The fact that less progress has been made in structural characterization of the racemate crystalline phases may be related to the fact that, in crystallization of racemic systems, the formation of a racemate crystalline phase competes with the alternative crystallization pathway leading to the formation of a conglomerate phase (i.e., a physical mixture of enantiomerically pure crystals of the R-enantiomer and enantiomerically pure crystals of the S-enantiomer). At the present time, there are five members of the family of amino acids for which no racemate crystal structure has been reported: asparagine, phenylalanine, threonine, arginine and lysine. In three of these cases, the formation of conglomerates on crystallization from racemic solutions has been reported, specifically for asparagine,[10] phenylalanine[7] and threonine.[11] Clearly, however, we cannot rule out the possibility that experimental conditions could be found under which DL-asparagine, DL-phenylalanine and DL-threonine would crystallize as racemates rather than conglomerates. To our knowledge, there have been no reports of the formation of non-solvate crystalline phases on crystallization from racemic solutions of DL-arginine and DL-lysine, although crystal structures have been reported for both monohydrate[12] and dihydrate[13] phases of DL-arginine. The present paper is focused on crystal structure determination of DL-arginine (non-solvate crystalline phase), which has been achieved by exploiting the opportunities provided by modern methods for analysis of powder XRD data, combined with periodic DFT-D calculations.

Although the task of determining crystal structures from powder X-ray diffraction (XRD) data is significantly more challenging than from single-crystal XRD data, advances over the past 20 years or so in techniques for analysis of powder XRD data[14-19] (particularly, the development of the direct-space strategy for structure solution) are such that the structural properties of organic materials of moderate complexity can now be determined from powder XRD data. In this regard, we note that there is growing interest[5,20-28] in utilizing periodic DFT calculations in conjunction with the analysis of powder XRD data, both for validation of the structural model and for enhancing

the quality of the structure at different stages of the structure determination process. The capability to determine the crystal structures of organic materials directly from powder XRD data has created considerable opportunities for structural characterization of materials prepared by processes that intrinsically generate microcrystalline powders as the product phase, including those prepared by solid-state desolvation (e.g., dehydration) processes.[3,5,6,29,30]

The opportunity to carry out structure determination of amino acids directly from powder XRD data is particularly advantageous in those cases for which hydrate phases are formed readily (for example, by incorporation of water from the atmosphere). In such cases, the anhydrous solid form is most readily accessed by solid-state dehydration of a hydrate phase. As such processes have a high propensity to produce the anhydrous phase as a microcrystalline powder, the only viable opportunity for crystal structure determination is the analysis of powder XRD data. This situation arises for both L-arginine and L-lysine, and thus powder XRD was essential for structure determination of the anhydrous phases in these cases.[3,5]

A similar situation applies in the case of DL-arginine (Figure 1), as both monohydrate[12] and dihydrate[13] solid forms of DL-arginine are known and the anhydrous form readily undergoes hydration in contact with atmospheric water. Indeed, one of the challenges in carrying out crystal structure determination of the anhydrous form of DL-arginine in the present work was to prevent hydration of the material during handling and measurement of the powder XRD data.

## Methods

DL-Arginine was purchased from Alfa Aesar as a polycrystalline powder, which was kept under dry conditions to prevent conversion to a hydrate form through exposure to atmospheric water. For powder XRD measurements, the sample was loaded into two glass capillaries which were then flame sealed. Powder XRD data were recorded at ambient temperature (21 °C) on a Bruker D8 Diffractometer (Ge-monochromated CuK$\alpha_1$ radiation) operating in transmission mode with a Våntec detector covering 3° in 2$\theta$. The powder XRD data[31] were recorded in the 2$\theta$ range from 4° to 50° (step size 0.017°). The total data collection time was 16 hours.

Unit cell determination was carried out using the program Crysfire,[32] which applies a range of different indexing algorithms to a set of peak positions measured from the powder XRD pattern. Profile fitting (using the Le Bail method[33]) and Rietveld refinement[34] were carried out using the program GSAS.[35] Structure solution was carried out using the direct-space strategy implemented in the program EAGER,[36-42] which is based on a genetic algorithm search procedure.

Periodic DFT-D calculations for geometry optimization were carried out (in conjunction with different stages of Rietveld refinement, as discussed below) using the program CASTEP[43] (Academic Release version 8.0). These calculations utilized ultrasoft pseudopotentials,[44] the PBE functional,[45] semiempirical dispersion corrections (TS correction scheme[46]), fixed unit cell, preserved space group symmetry, periodic boundary conditions, a basis set cut-off energy of 700 eV and a Monkhorst-Pack grid[47] of minimum sample spacing $0.05 \times 2\pi$ Å$^{-1}$.

**Structure Determination**

The powder XRD pattern of DL-arginine was indexed using the TREOR90 algorithm,[48] giving a unit cell with orthorhombic metric symmetry and unit cell axes of the following lengths: 5.37 Å, 9.20 Å, 18.26 Å. From the volume of the unit cell and consideration of density, the number of molecules in the unit cell was deduced to be $Z = 4$ (i.e., two molecules of L-arginine and two molecules of D-arginine). Profile fitting using the Le Bail technique led to an acceptable quality of fit for 23 combinations of orthorhombic space groups and different permutations of the unit cell axis lengths, and structure solution was attempted in each of these cases. In these structure solution calculations (discussed in more detail below), only space group $Pna2_1$ (with the following ordering of the unit cell axes: $a$ = 18.26 Å, $b$ = 5.37 Å, $c$ = 9.20 Å) yielded trial structures for which: (a) the arrangement of the molecules was structurally and chemically reasonable, and (b) a good fit to the experimental powder XRD data was achieved. The result from Le Bail fitting of the powder XRD data for this unit cell and space group is shown in Figure 2 ($2\theta$ range,[49] 7° to 50°; $R_{wp}$ = 1.95%, $R_p$ = 1.51%).

Structure solution was carried out using the direct-space strategy implemented using a genetic algorithm search technique in the program EAGER. For space group $Pna2_1$ with $Z = 4$, there is one molecule in the asymmetric unit ($Z' = 1$) and, in the direct-space structure solution calculations,

each trial structure was defined by a total of 11 structural variables (three positional, three orientational and five torsional). The tautomeric form of the molecule shown in Figure 1 was used, based on the reported crystal structure of L-arginine.[3] In total, 16 independent calculations were carried out, in each case for a population of 100 structures, with 40 mating and 30 mutation operations carried out per generation, and for a total of 100 generations. The trial structure giving the best fit to the experimental powder XRD data in each of the 16 calculations represented essentially the same structure and the trial structure with lowest $R_{wp}$ among all 16 calculations was used as the starting structural model for Rietveld refinement.[34] In the Rietveld refinement, standard restraints[50] were applied to bond lengths and bond angles, and planar restraints were applied to the carboxylate and guanidinium groups.

After the initial Rietveld refinement ($R_{wp} = 2.23\%$, $R_p = 1.64\%$), the structural model was subjected to geometry optimization using periodic DFT-D calculations (with fixed unit cell), which led to only a minor change in the molecular conformation. The resulting geometry optimized structure was then used as the starting structural model for a second stage of Rietveld refinement, which produced only very minor structural adjustments and a small improvement in the quality of fit. At the final stage of Rietveld refinement, an additional distance restraint was applied across the intermolecular N–H···O hydrogen bond involving the amine and carboxylate groups in the amino acid head groups of adjacent molecules (the periodic DFT-D calculations indicated that a rather long hydrogen bond is formed between these groups, as discussed below). The final Rietveld refinement[49] is shown in Figure 3 [$2\theta$ range, 7 to 50°; 2519 profile points; 95 refined variables; $R_{wp} = 2.21\%$, $R_p = 1.65\%$, $R_{wpbs} = 1.96\%$, $R_{pbs} = 1.81\%$, $\chi^2 = 1.613$ ($R_{wpbs}$ and $R_{pbs}$ are the background subtracted values of $R_{wp}$ and $R_p$, respectively)]. No corrections for preferred orientation were applied in the Rietveld refinement and analysis of the difference Fourier map generated from the final Rietveld refinement confirmed that there are no significant regions of electron density mismatch. The level of agreement between calculated and experimental powder XRD data achieved in the Rietveld refinement compares very favourably with that obtained in the Le Bail fitting procedure (Figure 2), leading to the conclusion that a Rietveld refinement of acceptable quality had been achieved.

**Results and Discussion**

The final refined crystal structure of DL-arginine is shown in Figures 4 and 5. The structure may be described in terms of a three-dimensionally connected array of intermolecular N–H···O hydrogen bonds, within which a number of well-defined hydrogen bonding motifs may be identified. First, chains of alternating L-arginine and D-arginine molecules propagate along the *a*-axis (horizontal in Figure 4, with one chain highlighted in cyan); within these chains, carboxylate and guanidinium groups in neighbouring molecules are linked by a double hydrogen-bonded ring designated $R_2^2(8)$ in graph set notation[51-52] (illustrated by the red circle in Figure 4). These chains are not straight but instead exhibit a zig-zag topology within the *ab*-plane (see Figure 5). Along the *b*-axis, adjacent zig-zag chains of this type are linked by a rather long, but very linear, N–H···O hydrogen bond (N···O distance, 3.64 Å; N–H···O angle, 175.9°; see Figure 5) involving the amine and carboxylate groups in the amino acid head-groups of molecules in adjacent chains. Along the *c*-axis, adjacent zig-zag chains are linked by further N–H···O hydrogen bonding, involving pairs of molecules (an example is highlighted in magenta in Figure 4) of the same chirality linked through three N–H···O hydrogen bonds, specifically: (a) at one end of each molecule, there are two N–H···O hydrogen bonds between the guanidinium group of one molecule and a carboxylate oxygen atom of the other molecule, giving rise to a cyclic motif (designated $R_2^1(6)$ in graph set notation; illustrated by the green circle in Figure 4) and (b) at the other end of each molecule, there is a single N–H···O hydrogen bond between guanidinium and carboxylate groups. Finally, a helical hydrogen-bonded chain running along the *b*-axis may also be identified (designated $C_4^2(8)$ in graph set notation; illustrated by the light blue curved arrow in Figure 4). This helical chain runs along a $2_1$ screw axis and the repeat unit, which involves four different molecules, is constructed from an alternation of guanidinium $NH_2$ groups and carboxylate oxygen atoms as follows: ···H–N–H···O···H–N–H···O. We note that all the N–H···O hydrogen bonds within this helical $C_4^2(8)$ chain motif are also present in one of the other hydrogen-bonding motifs discussed above.

Certain aspects of the crystal structure of DL-arginine resemble features in the crystal structure of L-arginine,[3] which also contains zig-zag chains in which adjacent molecules in the chain are linked by the same double hydrogen-bonded $R_2^2(8)$ ring motif involving guanidinium and carboxylate groups of adjacent molecules. The angle formed at the "bend" within the zig-zag chain

(defined as the angle between the planes containing the hydrogen-bonded groups) is higher for DL-arginine (102°) than L-arginine (76° and 81° for the two crystallographically independent chains). However, there are much more significant differences between the crystal structures of L-arginine and DL-arginine with regard to details of the hydrogen bonding *between* adjacent zig-zag chains. Significantly, in the crystal structure of L-arginine, the amine group in the amino acid head-group is engaged in three intermolecular hydrogen bonds (as the donor in two N–H···O hydrogen bonds and as the acceptor in one N–H···N hydrogen bond), whereas in the crystal structure of DL-arginine, this $NH_2$ group forms just one intermolecular hydrogen bond (as the donor in an N–H···O hydrogen bond) together with an intramolecular N–H···O hydrogen bond to a carboxylate oxygen atom in the same molecule. For comparison, Figure S1 (Supporting Information) shows the hydrogen-bonded chains of arginine molecules in the crystal structures of L-arginine and DL-arginine, as well as the hydrogen-bonded chains in the crystal structures of L-arginine dihydrate, DL-arginine monohydrate and DL-arginine dihydrate.

The crystal structures of DL-arginine and L-arginine both have four molecules in the unit cell, and as the unit cell volume is larger by 3.6% (at ambient temperature) for DL-arginine than for L-arginine, the density of DL-arginine is lower (1.29 g $cm^{-3}$ for DL-arginine and 1.34 g $cm^{-3}$ for L-arginine). Thus, arginine represents an exception to Wallach's rule,[53-54] which states that racemate crystalline phases have higher density than the enantiomerically pure crystalline phases of the same molecule. In 2012, Dunitz and Gavezzotti[55] showed that, of the 13 proteinogenic amino acids for which crystal structures of both the racemic and enantiomerically pure forms were known at that time, Wallach's rule is obeyed in eight cases and not obeyed in five cases. Our observation for arginine reported here further reinforces the conclusion that Wallach's rule does not apply to this class of materials.

**Concluding Remarks**

The crystal structure of DL-arginine reported in this paper provides further demonstration of the opportunities that now exist for determining the crystal structures of organic molecular materials by exploiting modern methods for analysis of powder XRD data. Clearly, this strategy enables structural knowledge to be obtained for materials that cannot be prepared as crystals of suitable size

and quality for single-crystal XRD. Furthermore, we emphasize the significant advantages of utilizing periodic DFT-D calculations at various stages within the structure determination protocol, both for validating the structural model derived from powder XRD data and for improving the accuracy of the structural model (for example, determining reliable positions of hydrogen atoms). We anticipate that the combined powder XRD/DFT-D strategy will also prove to be advantageous in structure determination in the remaining four cases of amino acids for which a (non-solvate) racemate crystal structure has not yet been reported, provided, of course, that experimental procedures can be found that lead to the formation of a racemate crystalline phase rather than a conglomerate in these cases.

## Supporting Information

Crystal information (cif) file for the crystal structure of DL-arginine. This information is available free of charge via the Internet at http://pubs.acs.org/

The experimental datasets for this work are available from the Cardiff University data catalogue at http://research.cardiff.ac.uk/***.

## AUTHOR INFORMATION

### Corresponding Author

* E-mail: HarrisKDM@cardiff.ac.uk

### Notes

The authors declare no competing financial interest.

## ACKNOWLEDGEMENTS

We are grateful to Cardiff University for financial support. We thank the École Nationale de Chimie, Physique et Biologie de Paris (Lycée Pierre-Gilles de Gennes) for providing a summer placement opportunity at Cardiff University to I.B. and the École Nationale Supérieure de Chimie de Clermont-Ferrand for providing a summer placement opportunity at Cardiff University to C.B., during which their contributions to this research project were carried out.

**References**


1. We note that one member (glycine) of this set of 20 amino acids is non-chiral. The other 19 amino acids in this set are chiral and are found to exist in nature only as the L-enantiomer.

2. Albrecht, G.; Corey, R. B. *J. Am. Chem. Soc.* **1939**, *61*, 1087-1103.

3. Courvoisier, E.; Williams, P. A.; Lim, G. K.; Hughes, C. E.; Harris, K. D. M. *Chem. Commun.* **2012**, *48*, 2761-2763.

4. Görbitz, C. H.; Törnroos, K. W.; Day, G. M. *Acta Crystallogr., Sect. B: Struct. Sci.* **2012**, *68*, 549-557.

5. Williams, P. A.; Hughes, C. E.; Harris, K. D. M. *Angew. Chem. Int. Ed.* **2015**, *54*, 3973-3977.

6. Williams, P. A.; Hughes, C. E.; Buanz, A. B. M.; Gaisford, S.; Harris, K. D. M. *J. Phys. Chem. C* **2013**, *117*, 12136-12145.

7. Ihlefeldt, F. S.; Pettersen, F. B.; von Bonin, A.; Zawadzka, M.; Görbitz, C. H. *Angew. Chem. Int. Ed.* **2014**, *53*, 13600-13604.

8. Dalhus, B.; Görbitz, C. H. *Acta Crystallogr., Sect. B: Struct. Sci.* **2000**, *56*, 720-727.

9. Minkov, V. S.; Tumanov, N. A.; Kolesov, B. A.; Boldyreva, E. V.; Bizyaev, S. N. *J. Phys. Chem. B* **2009**, *113*, 5262-5272.

10. Srisanga, S.; ter Horst, J. H. *Cryst. Growth Des.* **2010**, *10*, 1808-1812.

11. Sapoundjiev, D.; Lorenz, H.; Seidel-Morgenstern, A. *J. Chem. Eng. Data* **2006**, *51*, 1562-1566.

12. Kingsford-Adaboh, R.; Grosche, M.; Dittrich, B.; Lugerc, P. *Acta Crystallogr., Sect. C: Struct. Chem.* **2000**, *56*, 1274-1276.

13. Suresh, S.; Padmanabhan, S.; Vijayan, M. *J. Biomol. Struct. Dyn.* **1994**, *11*, 1425-1435.

14. Lightfoot, P.; Tremayne, M.; Harris, K. D. M.; Bruce, P. G. *J. Chem. Soc., Chem. Commun.* **1992**, 1012-1013.

15. Harris, K. D. M.; Tremayne, M.; Lightfoot, P.; Bruce, P. G. *J. Am. Chem. Soc.* **1994**, *116*, 3543-3547.

16. Chernyshev, V. V. *Russ. Chem. Bull.* **2001**, *50*, 2273-2292.

17. Tsue, H.; Horiguchi, M.; Tamura, R.; Fujii, K.; Uekusa, H. *J. Synth. Org. Chem. Jpn.* **2007**, *65*, 1203-1212.

18. David, W. I. F.; Shankland, K. *Acta Crystallogr., Sect. A: Found. Crystallogr.* **2008**, *64*, 52-64.

19. Harris, K. D. M. *Top. Curr. Chem.* **2012**, *315*, 133-178.

20. Seijas, L. E.; Mora, A. J.; Delgado, G. E.; López-Carrasquero, F.; Báez, M. E.; Brunelli, M.; Fitch, A. N. *Acta Crystallogr., Sect. B: Struct. Sci.* **2009**, *65*, 724-730.

21. van de Streek, J.; Neumann, M. A. *Acta Crystallogr., Sect. B: Struct. Sci.* **2010**, *66*, 544-558.

22. Dudenko, D. V.; Williams, P. A.; Hughes, C. E.; Antzutkin, O. N.; Velaga, S. P.; Brown, S. P.; Harris, K. D. M. *J. Phys. Chem. C* **2013**, *117*, 12258-12265.

23. van de Streek, J.; Neumann, M. A. *Acta Crystallogr., Sect. B: Struct. Sci. Cryst. Eng. Mater.* **2014**, *70*, 1020-1032.

24. Brooks, L.; Brunelli, M.; Pattison, P.; Jones, G. R.; Fitch, A. *IUCrJ* **2015**, *2*, 490-497.

25. Watts, A. E.; Maruyoshi, K.; Hughes, C. E.; Brown, S. P.; Harris, K. D. M. *Cryst. Growth Des.* **2016**, *16*, 1798-1804.

26. Gumbert, S. D.; Körbitzer, M.; Alig, E.; Schmidt, M. U.; Chierotti, M. R.; Gobetto, R.; Li, X.; van de Streek, J. *Dyes Pigments* **2016**, *131*, 364-372.

27. Hughes, C. E.; Reddy, G. N. M.; Masiero, S.; Brown, S. P.; Williams, P. A.; Harris, K. D. M. *Chem. Sci.* **2017**, *8*, 3971-3979.

28. Hempler, D.; Schmidt, M. U.; van de Streek, J. *Acta Crystallogr., Sect. B: Struct. Sci. Cryst. Eng. Mater.* **2017**, *73*, 756-766.

29. Guo, F.; Harris, K. D. M. *J. Am. Chem. Soc.* **2005**, *127*, 7314-7315.

30. Albesa-Jové, D.; Pan, Z.; Harris, K. D. M.; Uekusa, H. *Cryst. Growth Des.* **2008**, *8*, 3641-3645.

31. Another powder XRD pattern was recorded for DL-arginine over the extended data range $2\theta$ = 4° to 70°, and indicated that there is no significant diffraction data above $2\theta$ = 50°. As the powder XRD pattern (discussed in the text) recorded over the data range $2\theta$ = 4° to 50° was measured for a significantly longer time and had a superior signal/noise ratio, this powder XRD pattern was used in the structure determination calculations.

32. Shirley, R., *The CRYSFIRE System for Automatic Powder Indexing: User's Manual* The Lattice Press: Guildford, U.K., 1999.

33. Le Bail, A.; Duroy, H.; Fourquet, J. L. *Mat. Res. Bull.* **1988**, *23*, 447-452.

34. Rietveld, H. M. *J. Appl. Crystallogr.* **1969**, *2*, 65-71.

35. Larson, A.C.; Von Dreele, R.B. *Los Alamos National Laboratory Report* **2004**, LAUR 86-748.

36. Albesa-Jové, D.; Kariuki, B. M.; Kitchin, S. J.; Grice, L.; Cheung, E. Y.; Harris, K. D. M. *ChemPhysChem* **2004**, *5*, 414-418.

37. Kariuki, B. M.; Calcagno, P.; Harris, K. D. M.; Philp, D.; Johnston, R. L. *Angew. Chem. Int. Ed.* **1999**, *38*, 831-835.

38. Kariuki, B. M.; Psallidas, K.; Harris, K. D. M.; Johnston, R. L.; Lancaster, R. W.; Staniforth, S. E.; Cooper, S. M. *Chem. Commun.* **1999**, 1677-1678.

39. Cheung, E. Y.; McCabe, E. E.; Harris, K. D. M.; Johnston, R. L.; Tedesco, E.; Raja, K. M. P.; Balaram, P. *Angew. Chem. Int. Ed.* **2002**, *41*, 494-496.

40. Harris, K. D. M.; Habershon, S.; Cheung, E. Y.; Johnston, R. L. *Z. Kristallogr.* **2004**, *219*, 838-846.

41. Fujii, K.; Lazuen Garay, A.; Hill, J.; Sbircea, E.; Pan, Z.; Xu, M.; Apperley, D. C.; James, S. L.; Harris, K. D. M. *Chem. Commun.* **2010**, *46*, 7572-7574.

42. Fujii, K.; Young, M. T.; Harris, K. D. M. *J. Struct. Biol.* **2011**, *174*, 461-467.

43. Clark, S. J.; Segall, M. D.; Pickard, C. J.; Hasnip, P. J.; Probert, M. J.; Refson, K.; Payne, M. C. *Z. Kristallogr.* **2005**, *220*, 567-570.

44. Vanderbilt, D. *Phys. Rev. B: Condens. Matter* **1990**, *41*, 7892-7895.

45. Perdew, J. P.; Burke, K.; Ernzerhof, M. *Phys. Rev. Lett.* **1996**, *71*, 3865-3868.

46. Tkatchenko, A.; Scheffler, M. *Phys. Rev. Lett.* **2009**, *102*, 073005.

47. Monkhorst, H. J.; Pack, J. D. *Phys. Rev. B* **1976**, *13*, 5188-5192.

48. Werner, P.-E.; Eriksson, L.; Westdahl, M. *J. Appl. Crystallogr.* **1985**, *18*, 367-370.

49. The Le Bail fitting and Rietveld refinement calculations used the measured powder XRD data in the range $2\theta = 7°$ to 50°. The measured data in the range $2\theta = 4°$ to 7° were not used as no

peaks are present this range and as improved fitting of the baseline is achieved using only the range $2\theta = 7°$ to 50°.

50. Standard bond-length and bond-angle restraints were obtained from the mean values of similar structures deposited in the Cambridge Structural Database, as determined using the program Mogul (version 1.7) for bonds between non-hydrogen atoms. Bond-length restraints for bonds involving hydrogen atoms were taken from: Allen, F. H.; Kennard, O.; Watson, D. G.; Brammer, L.; Orpen, A. G.; Taylor, R. *J. Chem. Soc. Perkin Trans. 2* **1987**, S1-S19.

51. Etter, M. C. *Acc. Chem. Res.* **1990**, *23*, 120-126.

52. Etter, M. C.; MacDonald, J. C.; Bernstein, J. *Acta Crystallogr., Sect. B: Struct. Sci.* **1990**, *46*, 256-262.

53. Wallach, O. *Liebigs Ann. Chem.* **1895**, *286*, 119-143.

54. Brock, C. P.; Schweizer, W. B.; Dunitz, J. D. *J. Am. Chem. Soc.* **1991**, *113*, 9811-9820.

55. Dunitz, J. D.; Gavezzotti, A. *J. Phys. Chem. B* **2012**, *116*, 6740-6750.

**Figures**

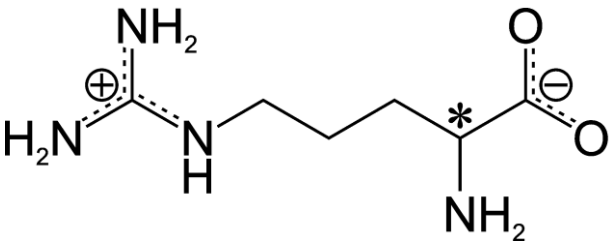


Figure 1. Molecular structure of arginine in the tautomeric form found in the known crystal structure of L-arginine[3] and in the crystal structure of DL-arginine reported here. The star indicates the stereogenic centre. L-Arginine is designated as the S-enantiomer and D-arginine is designated as the R-enantiomer.

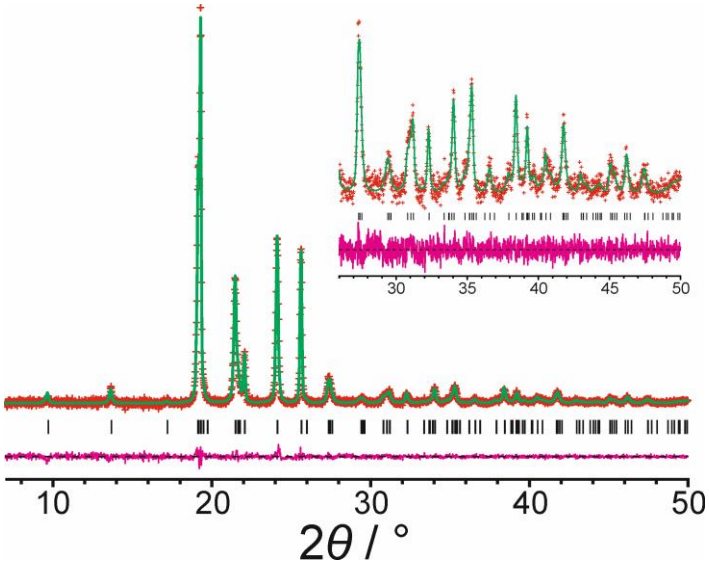


Figure 2. Le Bail fitting of the powder XRD data (with background subtracted) of DL-arginine (red + marks, experimental data; green line, calculated data; magenta line, difference plot; black tick marks, predicted peak positions).

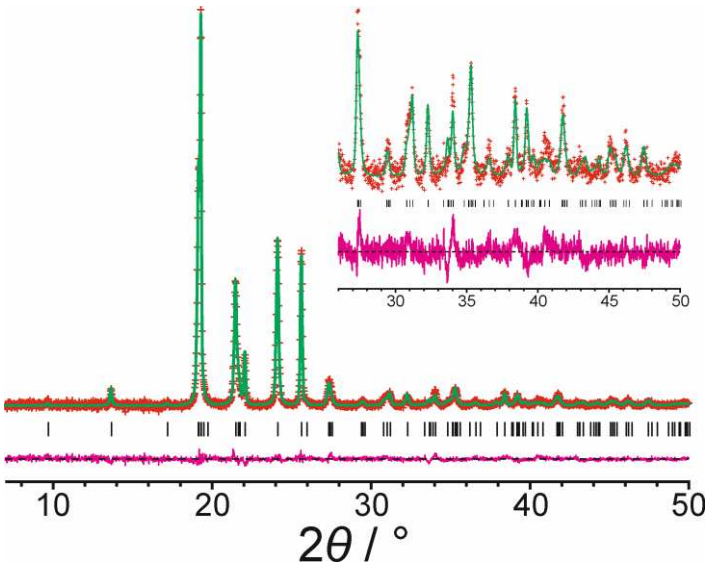


Figure 3. Final Rietveld refinement (with background subtracted) of DL-arginine (red + marks, experimental data; green line, calculated data; magenta line, difference plot; black tick marks, predicted peak positions).

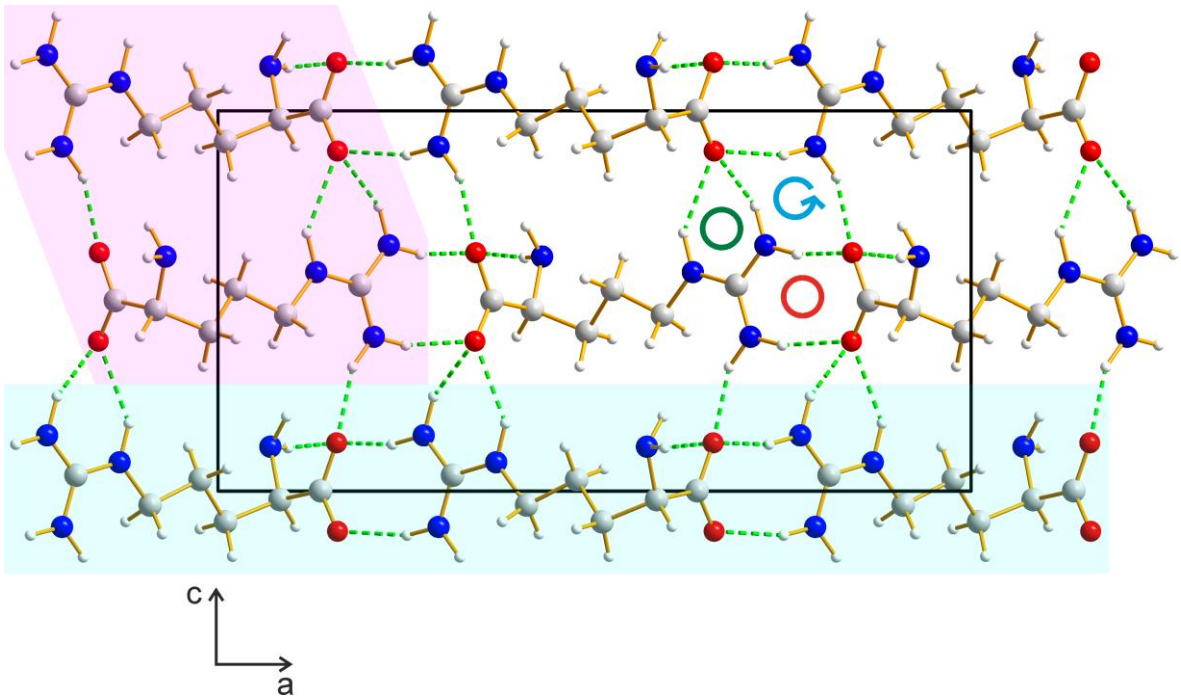


Figure 4. Crystal structure of DL-arginine viewed along the *b*-axis. Green dashed lines indicate hydrogen-bonding interactions. Chains of alternating D-arginine and L-arginine molecules propagate parallel to the *a*-axis (horizontal in the view shown, with one chain highlighted in cyan). These chains actually have a zig-zag topology, as evident when viewed along the *c*-axis in Figure 5. Adjacent molecules (of the same chirality) along the *c*-axis are also linked by hydrogen-bonding interactions (one pair of molecules is highlighted in magenta). Hydrogen-bonding motifs discussed in the text are indicated as follows: red circle, $R_2^2(8)$ ring; green circle, $R_2^1(6)$ ring; light-blue curved arrow, helical chain [ $C_4^2(8)$ ] running along the *b*-axis (into the plane of the page).

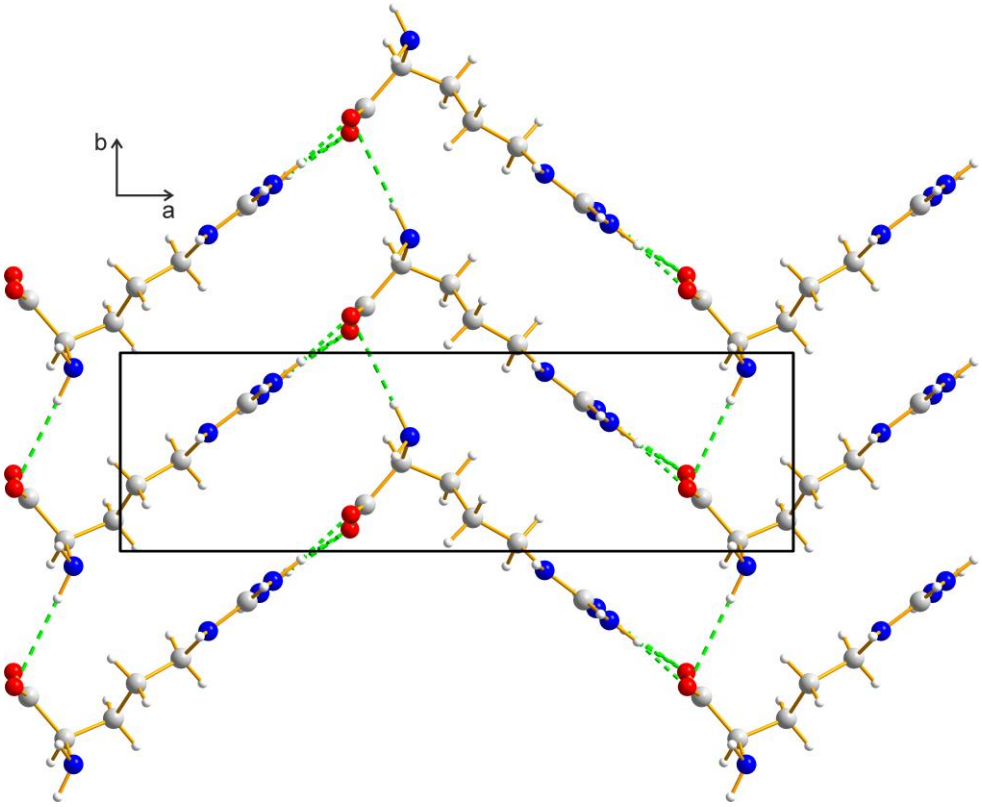


Figure 5. Crystal structure of DL-arginine viewed along the *c*-axis, showing three zig-zag chains propagating along the *a*-axis (horizontal). Green dashed lines indicate hydrogen-bonding interactions. Note that each molecule is engaged in an N–H···O hydrogen bond with a molecule in each of the two adjacent chains.